# Preliminary Walking Experiments with Underactuated 3D Bipedal Robot MARLO

Brian G. Buss[1], Alireza Ramezani[2], Kaveh Akbari Hamed[1], Brent A. Griffin[1], Kevin S. Galloway[3], Jessy W. Grizzle[1]

***Abstract*— This paper reports on an underactuated 3D bipedal robot with passive feet that can start from a quiet standing position, initiate a walking gait, and maintain an upright posture while traversing the length of the laboratory (approximately 11 m) at a speed of roughly 1 m/s. The controller was developed using the method of virtual constraints, a control design method first used on the planar point-feet robots Rabbit and MABEL. At the current stage of development, the robot's dynamic model has enough unknown parameters to preclude the use of optimization in the design of the virtual constraints. Here the virtual constraints were selected by hand to achieve robust planar walking, and then augmented with SIMBICON-inspired virtual constraints for the lateral stabilization. This resulted in unassisted 3D walking, both indoors and outdoors.**

## I. INTRODUCTION

This paper presents experimental results on underactuated 3D bipedal walking. The robot MARLO shown in Fig. 1 has walked both indoors and outdoors on passive prosthetic feet.

This research uses a 3D ATRIAS-series biped [1], [2] to inspire the development of control laws that naturally accommodate underactuation in bipedal locomotion. An important reason for studying underactuation is that even a fully actuated 3D robot can become underactuated when walking. The source of underactuation may be planned, as when seeking to execute a human-like rolling foot motion. The source of underactuation may also be unanticipated, such as when an uneven walking surface precludes three non-collinear points of contact, or even "worse", when the object under the foot rolls or causes slipping [3]. In each of these cases, the assumptions required for flat-footed ZMP-style walking are not met [4] and some other means is necessary for assuring a stable gait.

[1]Dept. of Electrical Engineering and Computer Science, [2]Dept. of Mechanical Engineering, University of Michigan, Ann Arbor, MI {bgbuss,aramez,kavehah,griffb,grizzle}@umich.edu

[3]Dept. of Electrical and Computer Engineering, United States Naval Academy, Annapolis, MD kgallowa@usna.edu

The vast majority of 3D bipedal robots use locomotion algorithms that require full actuation [5]–[9]. Important exceptions include PETMAN [10], M2V2 [11], COMAN [12], Denise [13], Biper-3 [14], and the Cornell biped [13]. The robot PETMAN is fully actuated but realizes an underactuated gait that includes heel strike, foot roll, and toe off, while responding impressively to lateral shoves; its control system is based on capture-points [10]. The bipedal robots M2V2 and COMAN are both underactuated due to series elastic actuation, and both have feet with ankles that are actuated in pitch and roll.

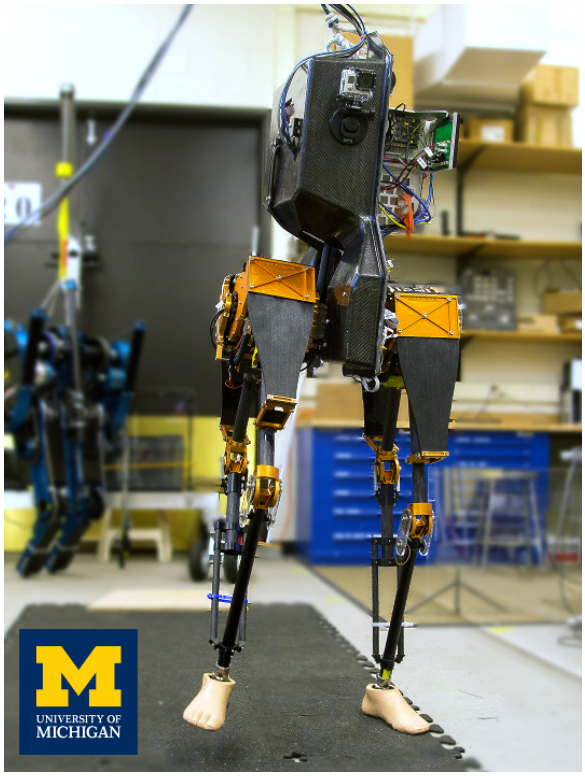


Fig. 1: MARLO is an ATRIAS 2.1 robot designed by Jonathan Hurst and the Dynamic Robotics Laboratory at Oregon State University. (Photo: Joseph Xu)

M2V2 excels at push recovery using capturability-based control [15]. While COMAN uses ZMP style walking, it is demonstrating improved energy efficiency and handles significant perturbations while standing. BIPER-3 was an early 3D biped which demonstrated dynamic balance; its feet made only point contact with the ground, so the machine was never statically stable. The Cornell biped and Denise are quasi-passive robots that use specially shaped feet to achieve lateral stability. It is hoped that the ATRIAS-series robots will prove to be significantly more energy efficient than PETMAN, and capable of more agile gaits than the other robots cited. This early-stage paper is far less ambitious, focusing on preliminary control results for 3D walking.

The feedback control law used here builds on previous work by the authors and colleagues for underactuated bipedal robots [16]. The method of virtual constraints has been extended to the 3D setting in [2], [17]–[19] and others. Extensive experimental work had been performed for underactuated planar gaits [16], [20]–[23], and reference [19] reported on the use of virtual constraints for an experimentally-realized fully actuated (flat-footed) 3D walking gait. This paper reports for the first time on underactuated walking in 3D using the method of virtual constraints.

The remainder of the paper is organized as follows. Section II provides a brief description of the robot used in the experiments. Section III summarizes the concept of virtual constraints as a control and gait design methodology; further details on these topics are available in [2], [24]. Section IV presents experiments in 2D locomotion that are aimed at using leg retraction [25], [26] to augment the robustness of the gait to perturbations. Section V describes a method for gait initiation in 3D; it allows the robot to stand quietly on passive prosthetic feet and then take a first step without any external assistance. Section VI presents experiments on 3D walking, where the gait is initiated from a standing position and converges to an average walking speed of $0.75$ m/s. Conclusions are given in Sect. VII.

## II. HARDWARE DESCRIPTION

MARLO is one of three robots in the ATRIAS series, built at Oregon State University. The robot is human-scale and highly underactuated. In particular, it has been designed to marry passive dynamics for energetic economy with active control for agility and robustness to disturbances. The floating body model has 16 DOF and 6 actuators. A full description is given in [2], [24].

### A. Bipedal mechanism

MARLO has two identical legs. The legs are very light and account for approximately $5\%$ of the total mass of the robot. Each leg is formed by a 4-bar parallelogram and hence includes two parallel shin links and two parallel thigh links. The left and right hips each house two brushless DC motors in series with 50:1 harmonic drives, the outputs of which are connected to the top two links of the respective 4-bar through large springs. In the frontal plane, the right and left hip units are connected to the torso through revolute joints with a common axis normal to the frontal plane. The hips are driven by brushless DC motors located at the top of the torso, acting through a gear ratio of 26.7:1. Each hip accounts for about 25% of the mass of the robot.

The torso accounts for approximately $40\%$ of the total mass of the robot and has room to house[1] the onboard real time computing, LiPo batteries, and power electronics for the motors. The overall mass of the robot is 55 Kg. For these experiments, the nominal point feet of the robot were replaced with commercial passive prosthetic feet. For the purposes of control design, a point foot model is assumed, with the caveat that the feet do provide some anti-yaw torque; see [2, Eqn. (5)].

### B. Coordinates

The orientation of the torso with respect to an inertial world frame can be described by three Euler angles $q_{zT}$, $q_{yT}$ and $q_{xT}$, referred to as the yaw, roll and pitch angles, respectively. In the sagittal plane, the angles of the shin and thigh links with respect to the torso frame are denoted by $q_{1R}$ and $q_{2R}$ for the right leg and $q_{1L}$ and $q_{2L}$ for the left leg, respectively. Since the shin and thigh links are driven by series-elastic actuators, the output shafts of the corresponding harmonic drive are additional DOF, denoted by $q_{gr1R}$ and $q_{gr2R}$ for the right leg and $q_{gr1L}$ and $q_{gr2L}$ for the left leg. Torques generated by the corresponding motors are denoted $u_{1R}$, $u_{2R}$, $u_{1L}$ and $u_{2L}$. In the frontal plane, the angles of the right and left hip motors with respect to the torso are $q_{3R}$ and $q_{3L}$, respectively, and the torques generated by the hip motors are denoted by $u_{3R}$ and $u_{3L}$.

In summary, the configuration variables during the single support phase can be expressed as

$$q := (q_{zT}, q_{yT}, q_{xT}, q_{1R}, q_{2R}, q_{1L}, q_{2L}, q_{gr1R}, q_{gr2R}, q_{3R}, q_{gr1L}, q_{gr2L}, q_{3L})^\top, \quad (1)$$

in which the first seven components are unactuated and the last six components are actuated. Furthermore, the

[1]For the experiments reported here, the real-time computer and the batteries were off board. The associated cables are visible in the videos.

control input vector is taken as

$$u := (u_{1R}, u_{2R}, u_{3R}, u_{1L}, u_{2L}, u_{3L})^\top. \tag{2}$$

Diagrams depicting these variables are available in [2].

### C. Embedded Control System and Sensing

Control algorithms for MARLO are implemented in MATLAB/Simulink and Stateflow. Real-time control is done with xPC Target. The control loop reads sensor data, computes control actions, and sends commands to actuators at a rate of 1 kHz. The yaw, roll and pitch angles of the torso frame are measured with a Microstrain MEMS-based inertial measurement unit (IMU) attached to the torso. Absolute encoders measure the angles $q_{1R}$, $q_{2R}$, $q_{1L}$, $q_{2L}$, $q_{gr1R}$, $q_{gr2R}$, $q_{gr1L}$ and $q_{gr2L}$. Incremental encoders mounted on the frontal-plane hip-actuation motors measure the hip angles $q_{3R}$ and $q_{3L}$. The real-time computer communicates with the motor amplifiers and sensors via an on-board EtherCAT network with custom EtherCAT slave devices.

MARLO does not have a camera. It presently lacks contact sensors at the leg ends to detect impacts. Impacts are detected by measuring the spring deflection in the series-elastic actuators driving the sagittal coordinates of the legs. A major upgrade in sensing is planned.

## III. CONTROL METHODOLOGY

Virtual constraints are a set of holonomic output functions defined in the configuration space of a mechanical system and zeroed through the action of a feedback control law. Virtual constraints are used to coordinate the links of the legged robot throughout a step, with the goal of inducing an asymptotically stable periodic walking gait. In its preferred implementation, the constraints are determined through model-based parameter optimization [2], [16], [18], [19]. Here, because the model of MARLO is not yet fully identified, they are designed by hand; see also [27] and [20]. A very brief summary of the methodology follows.

### A. Forming the constraints

The most basic form of the virtual constraints is

$$y := h(q) := h_0(q) - h_d(\theta(q)), \tag{3}$$

where $h_0(q)$ specifies the vector of variables to be controlled, $h_d(\theta)$ is the desired evolution of the controlled variables as a function of $\theta(q)$. A *gait-timing* variable or *mechanical-phase* variable $\theta(q)$ is used to replace time in parameterizing a motion of the robot. Consequently, $\theta(q)$ is selected to be strictly monotonic (increasing or decreasing) along nominal walking gaits.

As in Rabbit and MABEL, $\theta(q)$ is chosen as the angle of the virtual line connecting the stance ankle joint to the stance hip joint in the sagittal plane, i.e.,

$$\theta(q) := \begin{cases} \frac{\pi}{2} - q_{xT} - \frac{q_{1R}+q_{2R}}{2} & \text{in right stance} \\ \frac{\pi}{2} - q_{xT} - \frac{q_{1L}+q_{2L}}{2} & \text{in left stance.} \end{cases} \tag{4}$$

It is convenient to normalize $\theta(q)$ to the interval $[0, 1]$ and call it $s(q)$, as

$$s(q) := \frac{\theta(q) - \theta^+}{\theta^- - \theta^+}, \tag{5}$$

where $\theta^+$ and $\theta^-$ represent the values of $\theta$ at the beginning and end of a typical walking step.

A nominal set of controlled variables is

$$h_0(q_s) = \begin{bmatrix} q_{\text{LA},R} \\ q_{\text{LA},L} \\ q_{\text{KA},R} \\ q_{\text{KA},L} \\ q_{\text{Hip},R} \\ q_{\text{Hip},L} \end{bmatrix} = \begin{bmatrix} \frac{1}{2}(q_{gr1R} + q_{gr2R}) \\ \frac{1}{2}(q_{gr1L} + q_{gr2L}) \\ q_{gr2R} - q_{gr1R} \\ q_{gr2L} - q_{gr1L} \\ q_{3R} \\ q_{3L} \end{bmatrix}. \tag{6}$$

where $q_{\text{LA},i}$ is the leg angle (i.e., the angle between the torso and the line segment between the hip and the leg end), $q_{\text{KA},i}$ the knee angle, and $q_{\text{Hip},i}$ the hip angle of leg $i \in \{R, L\}$. The leg actuators act through springs, so we take leg angles and knee angles as the outputs of the harmonic drives. With this choice, the virtual constraints have vector relative degree two [16].

The desired evolution of the controlled variables $h_0(q)$ is chosen as

$$h_d(\theta) = B(s(\theta), \alpha) \tag{7}$$

where $B(s, \alpha)$ is a vector of Bézier polynomials in $s$ with coefficients $\alpha = \begin{bmatrix}\alpha_0 \cdots \alpha_M\end{bmatrix}$.

### B. Zeroing the outputs to impose the constraints

The outputs (3) are (approximately) zeroed to (approximately) impose the virtual constraints. With the model being poorly known, inverse dynamics is not used. Instead, more classical feedforward and PD control action is used,

$$u(q, \dot{q}) = u_{\text{FF}}(q, \dot{q}) + T(q) \left( \frac{K_D}{\varepsilon}\, \dot{y} + \frac{K_P}{\varepsilon^2}\, y \right). \tag{8}$$

The feed forward term $u_{\text{FF}}(q, \dot{q})$ primarily implements an approximate form of gravity compensation. The invertible matrix $T(q)$ in (8) relates the components of the output function $y(q)$ to the input variables $u$. The gains $K_P$ and $K_D$ are diagonal matrices, whereas $\varepsilon$ is a positive scalar to tune the settling time of the output.

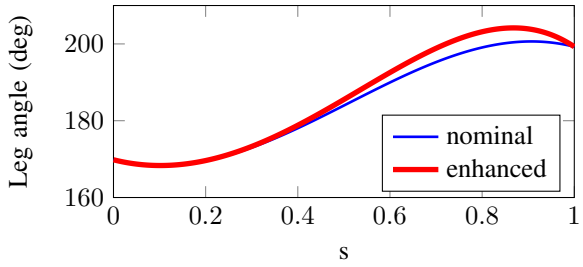


Fig. 2: Desired swing leg angles with and without enhanced swing leg retraction.

## IV. PLANAR WALKING AND LEG RETRACTION

Initial testing was performed with the robot attached to a boom which constrains the lateral motion of the torso. An encoder measuring the pitch angle of the torso was used instead of the IMU-derived pitch angle for some of the planar experiments. The purpose of these experiments was to identify and fix problems with the hardware, form an idea of the quality of the model, and develop a robust planar gait as a basis for 3D locomotion. The control design in this section uses the nominal controlled variables (6), with the desired (lateral) hip angles set to constants. The desired evolution of the virtual constraints in the sagittal plane was initially designed as in [2] on the basis of the CAD model of the robot, and then subsequently adjusted by hand to improve foot clearance; see the video [28]. The process of improving the robustness of this gait led to leg retraction, which is described next.

### A. Swing leg retraction

Humans and animals often brake or reverse the swing leg just before impact. This behavior, termed *swing leg retraction*, has been shown to improve stability robustness in spring-mass models of running [25].

We implement swing leg retraction by increasing the desired swing leg angle near the end of a step while leaving the final desired swing leg angle unchanged. Figure 2 compares the Bézier polynomials for the nominal and modified swing leg angle virtual constraints. The modified evolution was selected by adjusting a single Bézier coefficient and running a series of walking experiments during which the boom was occasionally pushed. More exaggerated leg retraction tended to cause the robot to "stomp" without noticeably improving stability robustness.

### B. Experimental results

Planar walking experiments confirmed that swing leg retraction enhanced disturbance rejection when walking

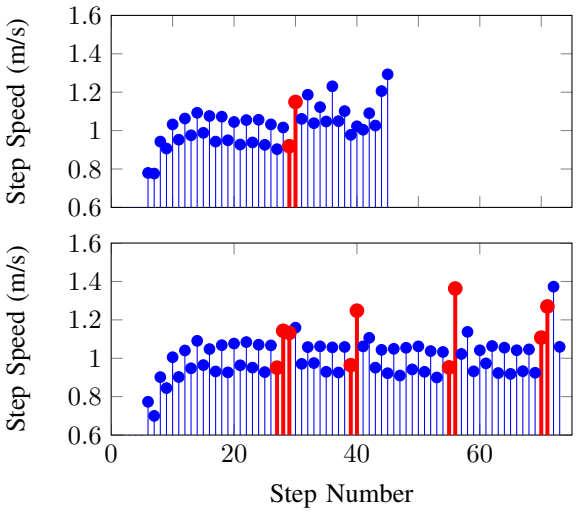


Fig. 3: Step speed during two experiments where the boom was pushed. Both experiments used point feet. In each plot, the heavy red stems indicate steps where the experimenter was in contact with the boom. Significant left-right asymmetry due to the boom appears in the period two oscillation in the step speed. (Top) Without enhanced swing leg retraction, the velocity increased after the push and remained higher than normal for multiple steps until the robot tripped and eventually fell. (Bottom) With enhanced swing leg retraction, the step velocity returns to nominal within about one step after the push. In this experiment the robot rejected multiple pushes before falling.

with point feet. External disturbances were induced by pushing on the boom as MARLO walked. The initial experiments were conducted on a circular boom, previously used for the robot MABEL [21]. Figure 3 shows the step speeds during two experiments (without and with enhanced swing leg retraction) where the boom was pushed from behind while the robot walked. With the nominal virtual constraint, the robot became unstable and eventually fell after a single mild push. With enhanced swing leg retraction, the robot rejected multiple pushes roughly increasing in intensity.

A second set of experiments was conducted in a new laboratory for 3D locomotion. In this set up, the boom was limited to a half circle. The desired knee angles were further modified to accommodate the prosthetic feet without scuffing. We verified that the control design remained stable and robust when the torso pitch encoder measurement was replaced with the lower bandwidth IMU-derived pitch angle, and when prosthetic feet were used instead of point feet. The robot successfully walked

over slightly uneven terrain while subjected to external disturbances; a video is available online [29].

## V. 3D GAIT INITIATION

Gait initiation consists of two parts, namely standing still, referred to here as quiet standing, and a transition step from quiet standing to a sustained walking motion. The strategy used here was developed in [24].

### A. Quiet standing

Imagine the robot standing on flat ground, in a fixed posture, with the torso upright and the legs parallel to the torso. Suppose further that the knees are bent approximately $20^\circ$ and the feet are flat on the ground. In this posture, the width of the stance is approximately $30$ cm, and the approximate left-right symmetry of the robot ensures that the lateral component of the CoM is between the feet, providing lateral static stability. Static stability in the sagittal plane is based on the following observation. Due to the feet being rigidly attached to the shin (i.e., lower front link of the 4-bar linkage), increasing the knee bend "raises" the heel, that is, it moves the CoP of the feet backward (i.e., toward the heel); on the other hand, straightening the knee "raises" the toe, that is, it moves the CoP forward.

It follows that as long as the nominal knee angle is not near the locking point, knee angle adjustment can be used to achieve a statically stable posture. This "passive" method of quiet standing was used in the experiments reported in Sect. VI. It is noted that active feedback stabilization of quiet standing was used in [24].

To exit quiet standing, it is enough to straighten the knees. The robot then pitches forward, rotating about the toes in the sagittal plane. The transition step can be triggered on the basis of pitch angular velocity.

### B. Transition step

A nominal standing posture is assumed, with the robot's CoM initially moving forward at $0.17$ m/s (roughly equivalent to the rotating about its toe at $10$ degrees per second). The mechanical phase variable (5) is used to parameterize a set of virtual constraints (3), with the controlled variables $h_0(q)$ given by (6). The desired evolution $h_d(\theta)$ of the virtual constraints is chosen to join "as closely as possible" the standing posture at $s = 0$ to the final posture at $s = 1$ of a periodic walking gait having an average walking speed of 0.75 m/s. In [24], this was posed as an optimization problem for choosing the coefficients in a set of Bézier polynomials in $h_d(\theta)$. Starting from the nominal polynomials reported in [24], we found it straightforward to adjust the final swing foot position on the first step in order to accelerate the robot into a forward walk.

### C. Sequencing

The transition step is initiated by the operator sending a ramp command to rapidly straighten the knees by a fixed amount, which pitches the robot forward. The commanded change in left knee angle is greater than the right so as to initiate a roll onto the right leg. When the IMU registers the torso pitching forward at $10$ degrees per second, the joint commands switch from constant set points to the virtual constraints. The robot rolls onto the right leg and steps forward with the left leg (see curves in [24] and video at [29]) At leg impact, control is passed to the steady-state walking controller described next.

## VI. 3D WALKING

Virtual constraints based on the controlled variables defined in (6) give rise to a periodic gait which is unstable [2], [18]. To achieve lateral stability we designed virtual constraints inspired by the SIMBICON balance control strategy [30]. SIMBICON and variations thereof have been used in simulation of a variety of legged creatures [31], [32] and in experiments with a quadrupedal robot [33]. We first summarize the original SIMBICON algorithm, then describe the modified version used in our experiments.

### A. Nominal SIMBICON algorithm

SIMBICON is a framework for the control of bipedal walking or running. It is based on a finite-state machine having a fixed target pose for each state. Within each state, PD control is used to drive individual joints toward the corresponding target angles. The swing hip and the torso angle are controlled relative to the world frame. The stance hip torque $\tau_A$ is computed from the torso torque $\tau_{torso}$ and the swing hip torque $\tau_B$ as $\tau_A = -\tau_{torso} - \tau_B$.

One additional element is needed to provide feedback for balance. The desired swing hip angle is updated continuously by a feedback law of the form

$$\psi_{sw,d} = \psi_{sw,d0} + c_p d + c_d \dot{d} \tag{9}$$

where $\psi_{sw,d}$ is the instantaneous target swing hip angle, $\psi_{sw,d0}$ is the nominal target swing hip angle specified by the state machine, and $d$ is the horizontal distance between the CoM and the stance ankle. The midpoint between the hips is used as an approximation of the CoM. In 3D, the nominal algorithm uses the same balance strategy in both the frontal and sagittal planes.

### B. Swing hip angle

The experiments reported in this paper use a modified form of SIMBICON to compute the desired swing hip angle in the lateral plane. We do not use SIMBICON in the sagittal plane. We define absolute hip angles

$$\psi_R = -q_{yT} - q_{3R} \tag{10}$$

$$\psi_L = q_{yT} - q_{3L} \tag{11}$$

so that both increase as the foot moves outward. We set $\psi_{st} = \psi_R$ and $\psi_{sw} = \psi_L$ in right stance; in left stance these definitions are reversed.

Instead of adjusting the desired swing hip angle based on the distance $d$ as in (9), we use the absolute stance hip angle $\psi_{st}$. This angle can be thought of as a linear approximation of $d$. The desired angle is

$$\psi_{sw,d} = \psi_{sw,d0} + c_p \psi_{st}, \tag{12}$$

where $\psi_{sw,d0}$ and $c_p$ are control parameters.

This strategy causes the swing leg to approximately mirror the stance leg in the lateral plane. One consequence of this strategy is that the swing foot generally moves *inward* during the beginning part of each step, and *outward* near the end. This is undesirable, as it brings the feet closer together during the middle of the step, increasing the likelihood that the feet will collide. It also increases tracking errors, particularly near the end of the step where they result in poor foot placement. We wish to modify (12) to reduce this inward motion.

It is also helpful to ensure that errors near the beginning of each step are relatively small. Doing so reduces unwanted yawing caused by large corrective torques before the new "swing" foot is off the ground.

We address both of these issues simultaneously. To reduce the inward motion of the swing foot we add a term to the right hand side of (12) which depends on the gait phase variable $s$. We also add a correction term which zeroes the error at $s = 0$ and vanishes as $s$ approaches one. The resulting expression for the desired swing hip angle is given by

$$\begin{aligned}\psi_{sw,d} = {} & (1-s)^3 \psi_{sw} - 3(1-s)^2 s \left(b_{sw} + a q_{yT}\right) \\ & + \left(3(1-s)s^2 + s^3\right)\left(\psi_{sw,d0} + c_p \psi_{st}\right)\end{aligned} \tag{13}$$

where $a = -1$ in right stance and $a = 1$ in left stance. The parameter $b_{sw}$ biases the value of $\psi_{sw,d}$ in the middle of a step in order to keep the feet apart. When $s = 0$ this equation gives $\psi_{sw,d} = \psi_{sw}$, and when $s = 1$ it reduces to (12). Note that (13) defines $\psi_{sw,d}$ as cubic Bézier polynomial in $s$. It differs from the desired evolutions introduced in Section III as the coefficients of the polynomial in (13) are updated continuously. To write the virtual constraint $0 = \psi_{sw,d} - \psi_{sw}$ in the form (3) we define

$$\begin{aligned}h_{0,sw}(q) = {} & \left(1 - (1-s)^3\right) q_{3,sw} - 3(1-s)^2 s b_{sw} \\ & + \left(3s^2 - 2s^3\right)\left(a(1+c_p) q_{yT} + \psi_{sw,d0} - c_p q_{3,st}\right).\end{aligned}$$

This quantity replaces $q_{3L}$ (in right stance) or $q_{3R}$ (in left stance) in (6); the corresponding element of $h_d(\theta)$ is set to zero.

### C. Torso control

Our method for controlling the torso also differs slightly from the SIMBICON strategy. Lateral torso control is easily accomplished by substituting a virtual constraint on the torso roll in place of the constraint on the stance hip. However, a satisfactory control design should also maintain the hip angles safely within their workspace. We make the tradeoff between torso and (relative) hip control explicit by defining a new actuated coordinate

$$h_{0,st}(q) = a\gamma q_{yT} + (1-\gamma)(q_{3,st} - b_{st}), \tag{14}$$

where $b_{st}$ is the desired stance hip angle, and $\gamma \in \mathbb{R}$. Note that $\gamma = 0$ corresponds to relative hip angle control (the nominal output function), while $\gamma = 1$ corresponds to pure torso control (as in SIMBICON). Setting $\gamma > 1$ causes the robot to lean the torso toward the stance foot, and $\gamma < 0$ causes the robot to lean the torso beyond the hip neutral position in the direction of the roll. The quantity $h_{0,st}(q)$ replaces $q_{3R}$ (in right stance) or $q_{3L}$ (in left stance) in (6); the corresponding element of $h_d(\theta)$ is set to zero.

The swing hip feedback torque is treated as a known disturbance on the torso. Its effect is canceled though disturbance feedforward, which can be implemented in the matrix $T(q)$ in (8). The same result is achieved in SIMBICON by the choice of $\tau_{stance}$.

### D. Experimental results

The revised lateral balance control strategy was introduced to find a baseline controller for 3D walking. Thus the initial goal in our 3D experiments was to get the robot to walk as far as possible. With the strategy described, the robot was able to walk the full length of the lab repeatedly.

Proper control of torso roll facilitates lateral swing foot placement. However, when the torso was controlled without regard for the stance hip angle, there were large oscillations in both hip angles. Setting $\gamma = 0.7$ in (14) led to a better compromise, with increased torso movement, but reduced hip oscillations. Figure 4 shows

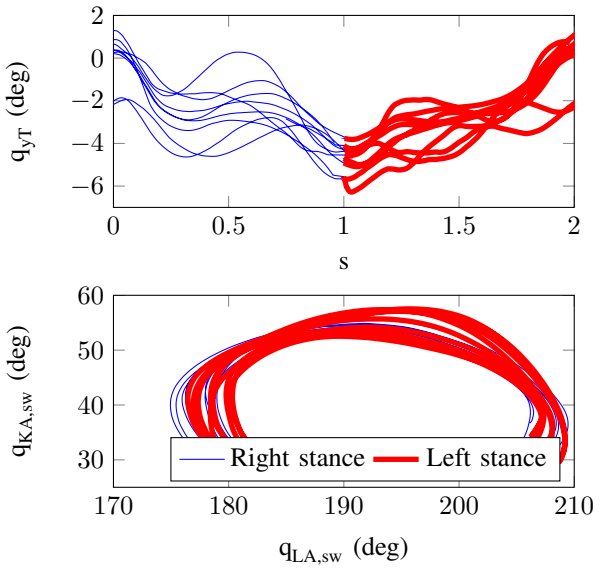


Fig. 4: 3D walking: (Top) Roll angle versus the gait timing variable, where $s$ is increased by 1 in left stance to show the 2-step periodic rocking motion. (Bottom) Swing knee angle versus swing leg angle.

the roll angle versus $s$ and the swing leg coordinates for the middle 8 seconds of a 3D walking experiment.

With the planar controller augmented with this modified form of SIMBICON for lateral control, the robot walked both indoors and outdoors. Snapshots from videos are shown in Fig. 5.

## VII. CONCLUSIONS

A hand-tuned control law based on virtual constraints was demonstrated to induce unassisted walking in a 3D bipedal robot having 12 degrees of freedom in single support and 6 actuators. The robot's sensor set consisted of a MEMS-based IMU and encoders at internal degrees of freedom. Foot impact was detected by deflection of large springs present in the series-elastic actuators that drive the 4-bar mechanism comprising the legs.

In the near future, the IMU will be upgraded and force-torque sensors will be installed at the passive ankles. With the enhanced sensing and motion capture, the parameters in the robot's mechanical model will be identified. Future control laws will be model based. The robot will be challenged with difficult outdoor environments.

## ACKNOWLEDGMENT

This material is based upon work supported by the National Science Foundation Graduate Student Research Fellowship under Grant No. DGE 1256260. A. Ramezani, B. Griffin, and J. W. Grizzle were supported by NSF grant ECCS-1231171. K. Akbari Hamed and K. Galloway were supported by DARPA Contract X0130A-B. Dennis Schweiger and Dennis Grimard contributed greatly to the design of the robotics laboratory used in this work. Jill Petkash, University of Michigan Orthotics and Prosthetics Center, and Todd Salley, College Park, assisted with the Tribute prosthetic feet used on the robot. Xingye (Dennis) Da assisted with the outdoor experiments. J. Grizzle thanks Russell Tedrake of MIT for hosting his sabbatical in early 2013, which gave rise to some of the ideas in this paper.

## REFERENCES

[1] J. Grimes and J. Hurst, "The design of ATRIAS 1.0 a unique monopod, hopping robot," *Climbing and walking Robots and the Support Technologies for Mobile Machines, International Conference on*, 2012.

[2] A. Ramezani, J. W. Hurst, K. Akbari Hamed, and J. W. Grizzle, "Performance Analysis and Feedback Control of ATRIAS, A Three-Dimensional Bipedal Robot," *Journal of Dynamic Systems, Measurement, and Control*, vol. 136, no. 2, Dec. 2013.

[3] IHMC Robotics Lab, "Atlas walking over randomness," Online: http://www.youtube.com/watch?v=d4qqM7_E11s, Nov 2013.

[4] A. Goswami, "Postural stability of biped robots and the foot-rotation indicator (FRI) point," *International Journal of Robotics Research*, vol. 18, no. 6, pp. 523–33, Jun. 1999.

[5] K. Hirai, M. Hirose, Y. Haikawa, and T. Takenake, "The development of Honda humanoid robot," in *Proc. of the IEEE International Conference on Robotics and Automation, Leuven, Belgium*, May 1998, pp. 1321–1326.

[6] J.-Y. Kim, I.-W. Park, and J.-H. Oh, "Experimental realization of dynamic walking of the biped humanoid robot KHR-2 using zero moment point feedback and inertial measurement," *Advanced Robotics*, vol. 20, no. 6, pp. 707–736, Jan. 2006.

[7] H. Yokoi, Kazuhito and Kanehiro, Fumio and Kaneko, Kenji and Fujiwara, Kiyoshi and Kajita, Shuji and Hirukawa, "Experimental Study of Biped Locomotion of Humanoid Robot HRP-1S," in *Experimental Robotics VIII*, ser. Springer Tracts in Advanced Robotics, B. Siciliano and P. Dario, Eds. Berlin, Heidelberg: Springer Berlin Heidelberg, Jun. 2003, vol. 5, ch. Experiment, pp. 75–84.

[8] T. Takenaka, "The control system for the Honda humanoid robot." *Age and ageing*, vol. 35 Suppl 2, pp. ii24–ii26, 2006.

[9] H.-o. Lim and A. Takanishi, "Biped walking robots created at Waseda University: WL and WABIAN family." *Philosophical transactions. Series A, Mathematical, physical, and engineering sciences*, vol. 365, pp. 49–64, 2007.

[10] G. Nelson, A. Saunders, N. Neville, B. Swilling, J. Bondaryk, D. Billings, C. Lee, R. Playter, and M. Raibert, "PETMAN: A humanoid robot for testing chemical protective clothing," *Journal of the Robotics Society of Japan*, vol. 30, no. 4, pp. 372–377, 2012.

[11] J. Pratt and B. Krupp, "Design of a bipedal walking robot," pp. 69 621F–69 621F–13, 2008.

[12] F. Moro, N. Tsagarakis, and D. Caldwell, "A human-like walking for the COmpliant huMANoid COMAN based on CoM trajectory reconstruction from kinematic motion primitives," in *Humanoid Robots (Humanoids), 2011 11th IEEE-RAS International Conference on*, 2011, pp. 364–370.

[13] S. H. Collins, A. Ruina, R. Tedrake, and M. Wisse, "Efficient bipedal robots based on passive-dynamic walkers," *Science*, vol. 307, pp. 1082–85, 2005.

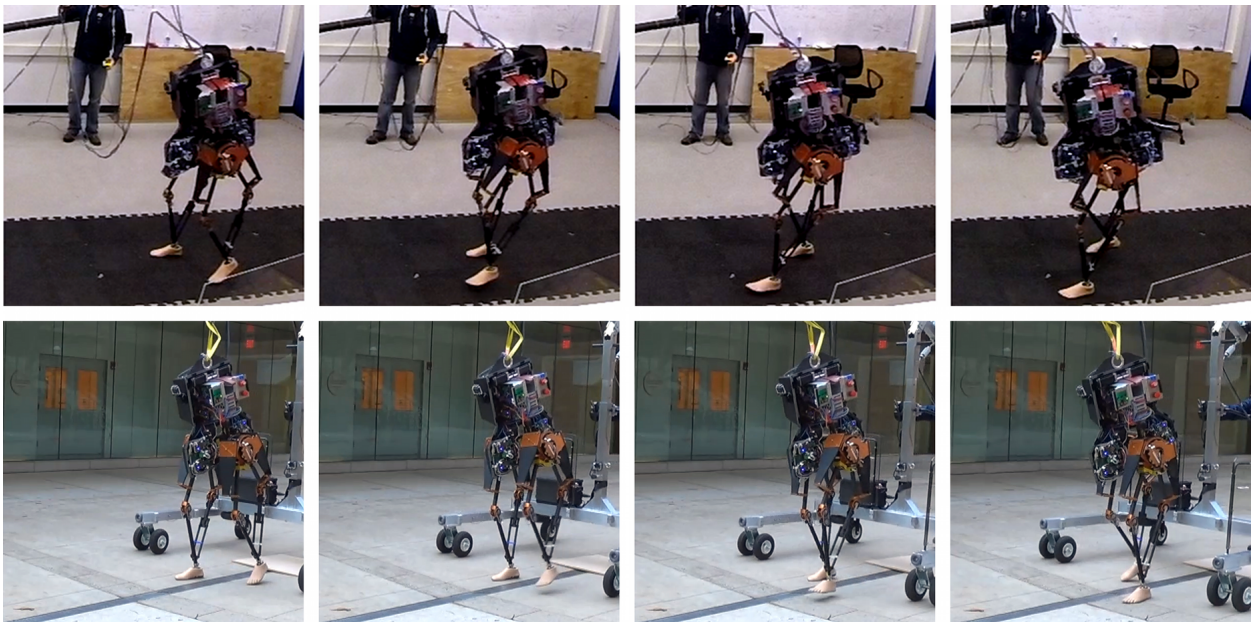

Fig. 5: Video snapshots from two 3D walking experiments. Frames are 200 ms apart. Videos of indoor (top row) and outdoor (bottom row) experiments are available online [29].


[14] H. Miura and I. Shimoyama, "Dynamic walk of a biped," *International Journal of Robotics Research*, vol. 3, no. 2, pp. 60–74, 1984.

[15] J. Pratt, T. Koolen, T. de Boer, J. Rebula, S. Cotton, J. Carff, M. Johnson, and P. Neuhaus, "Capturability-based analysis and control of legged locomotion, Part 2: Application to M2V2, a lower-body humanoid," *The International Journal of Robotics Research*, vol. 31, no. 10, pp. 1117–1133, Aug. 2012.

[16] E. R. Westervelt, J. W. Grizzle, C. Chevallereau, J. Choi, and B. Morris, *Feedback Control of Dynamic Bipedal Robot Locomotion*, ser. Control and Automation. Boca Raton, FL: CRC Press, June 2007.

[17] A. D. Ames and R. D. Gregg, "Stably extending two-dimensional bipedal walking to three," in *American Control Conference*, New York, U.S.A., Jul. 2007, pp. 2848–2854.

[18] C. Chevallereau, J. Grizzle, and C. Shih, "Asymptotically stable walking of a five-link underactuated 3D bipedal robot," *IEEE Transactions on Robotics*, vol. 25, no. 1, pp. 37–50, February 2009.

[19] A. D. Ames, E. A. Cousineau, and M. J. Powell, "Dynamically stable robotic walking with NAO via human-inspired hybrid zero dynamics," in *Hybrid Systems, Computation and Control (HSCC)*, Philadelphia, April 2012.

[20] J. W. Grizzle, G. Abba, and F. Plestan, "Asymptotically stable walking for biped robots: Analysis via systems with impulse effects," *IEEE Transactions on Automatic Control*, vol. 46, no. 1, pp. 51–64, Jan. 2001.

[21] K. Sreenath, H. Park, I. Poulakakis, and J. Grizzle, "A compliant hybrid zero dynamics controller for stable, efficient and fast bipedal walking on MABEL," *International Journal of Robotics Research*, vol. 30(9), pp. 1170–1193, 2011.

[22] K. Sreenath, H.-W. Park, and J. Grizzle, "Design and experimental implementation of a compliant hybrid zero dynamics controller with active force control for running on MABEL," in *Int. Conf. on Robotics and Automation (ICRA)*, May 2012.

[23] H.-W. Park, K. Sreenath, A. Ramezani, and J. Grizzle, "Switching control design for accommodating large step-down disturbances in bipedal robot walking," in *Int. Conf. on Robotics and Automation (ICRA)*, May 2012.

[24] A. Ramezani, "Feedback control design for MARLO, a 3D-bipedal robot," PhD Thesis, University of Michigan, 2013.

[25] A. Seyfarth, H. Geyer, and H. Herr, "Swing leg retraction: A simple control model for stable running," *Journal of Experimental Biology*, vol. 206, pp. 2547–2555, 2003.

[26] D. G. E. Hobbelen and M. Wisse, "Swing-leg retraction for limit cycle walkers improves disturbance rejection," *Robotics, IEEE Transactions on*, vol. 24, no. 2, pp. 377–389, 2008.

[27] J. Grizzle, J. Hurst, B. Morris, H. Park, and K. Sreenath, "MABEL, a new robotic bipedal walker and runner," in *American Control Conference*, St. Louis, Missouri, June 2009.

[28] Dynamic Leg Locomotion and Oregon State DRL, "ATRIAS 2.1 First Steps," Online, Sept 2012.

[29] J. W. Grizzle. Dynamic Leg Locomotion. Youtube Channel: http://www.youtube.com/DynamicLegLocomotion.

[30] K. Yin, K. Loken, and M. van de Panne, "SIMBICON: Simple biped locomotion control," *ACM Transactions on Graphics*, vol. 26, no. 3, 2007.

[31] S. Coros, A. Karpathy, B. Jones, L. Reveret, and M. van de Panne, "Locomotion skills for simulated quadrupeds," *ACM Transactions on Graphics*, vol. 30, no. 4, pp. 59:1–59:12, 2011.

[32] T. Geijtenbeek, M. van de Panne, and A. F. van der Stappen, "Flexible muscle-based locomotion for bipedal creatures," *ACM Transactions on Graphics*, vol. 32, no. 6, 2013.

[33] C. Gehring, S. Coros, M. Hutter, M. Bloesch, M. Hoepflinger, and R. Siegwart, "Control of dynamic gaits for a quadrupedal robot," in *Robotics and Automation (ICRA), 2013 IEEE International Conference on*, 2013, pp. 3287–3292.